EAI Endorsed Transactions
on Industrial Networks and Intelligent Systems
Research Article EAI.EU

Improving Performance of the Typical User in the Indoor Cooperative NOMA Millimeter Wave Networks with Presence of Walls

Sinh Cong Lam[1,*], Xuan Nam Tran[2]

[1]Faculty of Electronics and Telecommunications, VNU - University of Engineering and Technology
[2]Advanced Wireless Communications Group, Le Quy Don Technical University

Abstract

The beyond 5G millimeter-wave cellular network system is expected to provide high-quality service in indoor areas. Due to the high density of obstacles, cooperative communication techniques are employed to improve the user's desired signal power by finding more than one appropriate station to serve that user. While the conventional system utilizes additional equipment such as Reconfigurable Intelligent Surfaces (RIS) and relays to enable cooperative features, the paper introduces a new network paradigm that utilizes the second nearest Base Station (BS) of the typical user as the Decode and Forward (DF) relay. Thus, depending on the success of decoding the message from the user's serving BS or the second nearest BS, the typical user can work with or without assistance from the relay, whose operation follows the discipline of the power-domain NOMA technique. In the case of relay assistance, the Maximum Ratio Combining technique is utilized by the typical user to combine the desired signals. To examine the performance of the proposed system, the Nakagami-m and the newly developed path loss model, which considers the density of walls and their properties, are adopted to derive the coverage probability of the user with and without relay assistance. The closed-form expressions of this performance metric are derived using Gauss quadrature and Welch-Satterthwaite approximation. Through analytical and simulation results, it is seen that the proposed system can improve the user coverage probability by up to 10%.

Received on 20 February 2024; accepted on 05 April 2024; published on 08 April 2024

Keywords: Cooperative Communication, Non-orthogonal Multiple- Access, Beyond 5G, Poisson Point Process

doi:10.4108/eetinis.v11i2.5156

The recent breakneck speed of the high quality of services demand is pushing the deployment of millimeter wave band in B5G cellular networks. Due to the weak penetration ability and fast attenuation, the millimeter wave is usually recommended to provide the coverage in indoor and outdoor small areas such as events, stadiums, and indoor offices. To study the feasibility of the millimeter wave in the coverage provision, various works have focused on finding the appropriate path loss model for these bands. As specified in 3GPP document [1], the path loss model, which is a mix of Light-of-Sight (LoS) and non-Light-of-Sight (nLoS) scenarios, is a potential model to compute the loss of power over distances. Utilization of the mixed LoS/nLoS model was employed in various works such as [2–4]. In [4], the performance of the cellular network with the nearest and strongest BS association schemes was evaluated as a function of the BS height. The Free Cell Massive Multi-Input Multi-Output (MIMO) performance was also examined under the effects of LoS/nLoS scenarios in References [2, 3]. In another work [5], the LoS/nLoS path loss model was utilized to examine the performance of the 5G X-duplex multi-relay system. In recent work [6], the different layouts of walls and their properties such as distribution, length, and penetration loss were studied in terms of modeling and performance evaluation. By comparing the network performance of different network layouts, the paper derived the suitable

*Corresponding author. Email: congls@vnu.edu.vn

mathematical expression of LoS/nLoS probability and path loss that captures the main properties of walls.

Although the mmWave band can provide a huge available bandwidth for each user, the heavy penetration loss of this band requires additional techniques that can improve the desired signal strength. In that context, cooperative communication is used as the key technique of the B5G cellular system to allow each user to simultaneously have connections to more than one stations [7]. Conventionally, the cooperative communication technique can be employed by exploring the existing network infrastructure, i.e. Coordinated Multi-Point Processing (CoMP) [8], or deploying the additional hardware such as Reconfigurable Intelligent Surface (RIS) or relays [9]. CoMP and relays have been introduced for previous cellular systems and mentioned by 3GPP as the fundamental elements of these systems [8]. Currently, both CoMP and relays are studied with new features to adapt to advanced techniques of B5G such as Non-Orthogonal Multi-Access (NOMA) [10], beam forming [11], massive MIMO and Simultaneous Wireless Information and Power Transfer (SWIPT)[12]. The operation of CoMP in the industrial 5G network was also studied to provide Ultra-Reliability and Low Latency (URLLC) service. In addition, the combination of deployment of relays in the CoMP network was also studied [13, 14]. In these above works, it was proved that the CoMP deployment can significantly improve the spectrum efficiency and system performance. While CoMP and relays are well-known applications of the cooperative communication technique in the 4G cellular systems, RIS has been recently introduced in 5G systems as a new candidate support equipment that can work as the Amplify and Forward relay but with lower installation cost and power consumption. The feasibility of RIS deployment has been demonstrated in both theoretical and practical aspects. Regarding to theoretical aspect, the authors in the system with RIS can significantly improve the typical user performance [15–17]. Furthermore, RIS can work with other B5G techniques such as massive MIMO [18, 19], full-duplex technique [20]. Regarding to practical aspect, the RIS-assisted network architecture and RIS design were investigated in [21, 22].

From the above analysis, the deployment of cooperative communication for B5G cellular system is a defined trend. Although non-additional hardware is required, the utilization of CoMP has very high requirements for backhaul links such as very large bandwidth, the frequency and phase synchronization of 50 parts per billion (ppb) and 1.5 μs [23]. In addition, backhaul overload is also a big challenge in the CoMP cellular network [24, 25]. Thus, most studies work on the utilization of additional equipment such as RIS and relay as the potential deployment of cooperative communication. In our recent work [26], a cooperative NOMA network system in which each cell edge user is served by both its nearest and second nearest BSs. In such a system, the nearest BS is called the primary serving BS while the second nearest one acts as the Amplify and Forward relay. The analytical results under the Stretched Path Loss Model show that the proposed system can provide a higher user performance but consume less power. However, the typical user in that paper utilizes the selection combination technique to receive multiple signals from the serving BS and relay. Particularly, the typical user only takes the strongest signal for further processing. Based on the success of that model, this paper proposes a model for the indoor millimeter wave B5G cellular network where the second nearest BS works as the Decode and Forward relay of the typical user. To determine the transmission power and the operational band of the relay, the NOMA technique is used together with Successive Interference Cancellation (SIC) to improve the spectrum efficiency and suppress interference. In stead of utilizing antenna selection technique at the typical user, this paper assumes the typical user combines two desired signals from the serving BS and relay by the meaning of Maximum Ratio Combining (MRC) which can provide a significantly higher performance than the antenna selection technique [27]. Furthermore, to examine the performance of the proposed system model, the newly developed path loss model, which was discussed in the first paragraph of this section, is adopted [6].

Generally, the remarkable contributions of this paper against aforementioned work is highlighted the following aspects:

- Unlike the related work that uses the separated equipment to work as the Decode and Forward (DF) relays, this paper utilizes the second nearest BS of the typical user as the relay. Specifically, the relay operates according to the policy of power-domain NOMA. In this scheme, the serving BS and the relay of the typical user operate on the same frequency band, with the relay transmitting at a lower power level than the serving BS to avoid interference. The utilization of the second nearest BS as the relay for the typical user can significantly reduce the installation and running costs, especially for the indoor environment where may not have enough free space to separately install both BS and relay stations.

- The coverage probability expressions of the typical user with and without relay assistance in the proposed system model are derived in the indoor wireless transmission condition with the presence of walls. In addition, the small-scale fading between the typical user and its associated station (serving BS and relay) follow Nakagami-m

distribution while the small-scale fading between the typical user and interfering BSs are ignored in performance analysis to obtain the lower bound performance. By utilizing the meaning of Gauss quadrature, the closed-form expressions for the typical user coverage probability are conducted.

Through the analytical results that examine the effects of density of walls and BSs on the typical user coverage probability, it can be stated that the typical user in the proposed system can achieve a coverage probability of a 10% higher than another in the conventional system.

1. System model

In this paper, an indoor B5G millimeter wave cellular network where averagely λ BSs are deployed according to Spatial Poisson Point Process (PPP) distribution in every m^2 service area while the UE is at the origin.

To enhance the performance without the additional hardware deployment, the paper assumes that the second nearest BS of the typical user acts as the DF relay to decode the signals from the cooperative BS and forward them to this user. Thus, the typical user directly communicates with its nearest BS (serving BS) and the second nearest BS (relay) as in Figure 1. Let $r^{(k)}$ is the distance from the typical user to BS k; $\phi^{(k)}$ is the angle between the horizontal axis of the Cartesian coordinate system and the vector that starts from the origin and ends at the position of BS k. Thus, the location of BS k in the Cartesian coordinate system is $\left(r^{(k)}\cos\phi^{(k)}, r^{(k)}\sin\phi^{(k)}\right)$. For better readability, let $k = bu$ and $k = ru$ correspond to the nearest BS, i.e. serving BS, and the second nearest BS, i.e. the relay, of the typical user. As illustrated in the related works [28], the joint Probability Density Function (PDF) $r^{(bu)}$ and $r^{(ru)}$ is determined by

$$f_{12}\left(r^{(bu)}, r^{(ru)}\right) = (2\pi\lambda)^2 r^{(bu)} r^{(ru)} \exp\left(-\pi\lambda\left[r^{(ru)}\right]^2\right) \quad (1)$$

The distance between the serving BS of the typical user and BS k is computed as follows

$$r_k^{(b)} = \sqrt{\left[r^{(bu)}\right]^2 + \left[r^{(k)}\right]^2 - 2r^{(bu)}r^{(k)}\cos\left[\phi^{(bu)} - \phi^{(k)}\right]} \quad (2)$$

Since the BSs are uniformly distributed in both vertical and horizontal axis, $\phi^{(bu)}$ and $\phi^{(k)}$ are uniform random variables in a range of $[0, 2\pi]$. Thus, letting $\Phi^{(k)} = |\phi^{(bu)} - \phi^{(k)}|$, then the PDF of $\Phi^{(k)}$ is

$$f_\Phi(\Phi^{(k)}) = \frac{2\pi - \Phi^{(k)}}{2\pi^2}; \quad 0 \le \Phi^{(k)} \le 2\pi \quad (3)$$

With assistance from the relay, the operation of the proposed system is described by two consecutive phases:

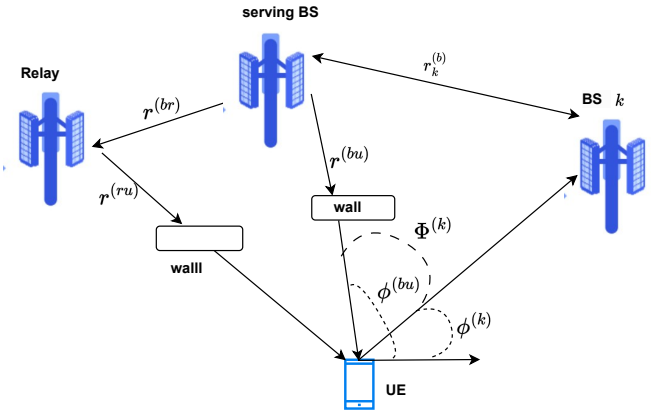

Figure 1. System model

- During the first phase, the typical user identifies its nearest and second nearest BSs. After that, it sends signaling messages to these BSs to ask the nearest BS for service provision and the second nearest for communication assistance.
- During the second phase, the selected relay performs the functions of a receiver to obtain the transmitted messages from the serving BS.
  - If the relay successfully decodes the received messages, it re-modulates and forwards the decoded messages to the typical user. Thus, the typical user simultaneously receives two desired signals from the serving BS and relay.
  - If the relay is unable to detect the received messages, it sends a feedback message to both serving BS and typical user to refuse the assistance request. Thus, the typical user only receives the desired signal from the serving BS.

1.1. Downlink SINR

Desired signal power

In this section, the downlink SINR of the typical user in two cases, where the relay successfully and unsuccessfully decodes the messages from the serving BS, are discussed.

During *the first phase*, the BS transmits its signals to the typical user and its relay using different antennas. Particularly,

- The first antenna utilizes a transmission power of $P^{(b)}$ and towards the typical user location. The power of the received signal at the typical user is

$$S^{(bu)} = P^{(b)} g^{(bu)} L\left(r^{(bu)}\right) \quad (4)$$

where $g^{(bu)}$ is power gains of the channel from the BS to the typical user; $L\left(r^{(bu)}\right)$ are the corresponding path loss.

- The second antenna has the responsibility to transmit the signals to the relay at the same power $P^{(b)}$ as to serve the typical user. It is also assumed that the BSs exchange information together on the special bands to avoid intercell interference. Thus, the signal power and Signal-to-Noise Ratio (SNR) at the relay from the serving BS of the typical user is

$$S_b = P^{(b)} g^{(b)} L\left(r^{(br)}\right) \tag{5a}$$

$$SNR^{(br)} = \frac{S_b}{\sigma^2} \tag{5b}$$

where σ^2 is the Gaussian noise power.

At the initial event of *the second phase*, the relay decodes the received signal to obtain the transmitted message which is possible if its received SINR is greater than the minimum required value. Let T_r as the minimum value of SNR, that the relay requires to successfully decode the messages. The event and the corresponding probability that the relay successfully decodes the received signal is

$$SNR^{(br)} > T_r \quad \text{and} \quad \mathcal{P}_r = \mathbb{P}\left(SNR^{(br)} > T_r\right) \tag{6}$$

Without relay assistance In this case, the relay is unable to decode the received messages from the serving BS. The typical user only receives the desired signal from the serving BS. The downlink signal power is formulated as follows

$$S^{(bu)} = P^{(b)} g^{(bu)} L(r^{(bu)}) \Big| SNR^{(br)} < T_r \tag{7}$$

With relay assistance After successfully decoding the messages from the serving BS, the relay forwards the decoded messages on the secondary sub-band to typical user with a power of $P^{(ru)}$. Hence, the received signal power $S^{(ru)}$ of the typical user from the relay can be re-written in the form of the following conditional event

$$S^{(ru)} = P^{(ru)} g^{(ru)} L\left[r^{(ru)}\right] \Big| SNR^{(br)} > T_r \tag{8}$$

where $g^{(ru)}$ and $L\left[r^{(ru)}\right]$ are the channel power gain and path loss from the typical user to its relay.

In this case, the typical user simultaneously receives signals from the serving BS and relay. By utilizing the Maximum Ratio Combining technique, the total received signal power at the typical user in this case is

$$\left(S^{(ru)} + S^{(bu)}\right) \Big| SNR^{(br)} > T_r \tag{9}$$

Consequently, the downlink SINR of the typical user is obtained by

$$\begin{cases} SINR^{(wr)} = \dfrac{\left(S^{(ru)} + S^{(bu)}\right)}{I + \sigma^2} \Big| SNR^{(br)} > T_r \\ SINR^{(or)} = \dfrac{S^{(bu)}}{I + \sigma^2} \Big| SNR^{(br)} < T_r \end{cases} \tag{10}$$

where I is the total interference on a typical sub-band, which is computed in the next paragraphs.

Interference power

Since the BS transmits on a given sub-band at two power levels to serve two different users, e.g. $P^{(ru)}$ when it acts as a relay and $P^{(b)}$ when it works as the primary serving BS. Thus, the power-domain NOMA technique is utilized at the relay to determine the appropriate transmission power and the Successive Interference Cancellation (SIC) technique is required at the typical user to suppress interference from its serving BS and relay, and detect the desired signal. To minimize impacts on the performance of relay function utilization, the transmission power of the relay is usually smaller than that of BS, i.e. $P^{(b)} > P^{(ru)}$.

Due to sharing the bandwidth between all BSs, the typical user is affected by interfering from all BSs that transmit on the same sub-band with the serving BS of the typical user. In addition, the relays also transmit on the same sub-band with the BSs that they assist. Consequently, each adjacent BS can create interference to the typical user through two different signals which are generated when the BS serves its active users and works as the relay to assist the user at the neighboring cell, respectively. Hence, the total interference of the typical user is

$$I = \sum_{k \in \theta^{(r)}} P^{(ru)} g_k^{(ru)} L(r_k^{(ru)}) + \sum_{h \in \theta^{(b)}} P^{(b)} g_h^{(bu)} L(r_h^{(bu)}) \tag{11}$$

where $\theta^{(r)}$ and $\theta^{(b)}$ are the set of interfering relays and BSs whose transmission powers are $P^{(ru)}$ and $P^{(b)}$, respectively; the wireless channels from the typical user to its relay and serving BS are respectively characterized by the instantaneous power gains $g_k^{(ru)}$ and $g_k^{(bu)}$, and the distances $r_k^{(ru)}$ and $r_k^{(ru)}$.

1.2. Small-Scale fading and Large-Scale fading

In wireless communication, the user can estimate the small-scale fading of the wireless channel between its self and its associated station but it is unfeasible for the user to estimate the small-scale fading to the adjacent BSs. Thus, this paper only takes the small-scale fading from the user to its serving station (serving BS and relay), and ignores the small-scale fading from the user

to the adjacent BSs. By this way, we can obtain the lower bound performance of the typical user.

Due to the generalization of Nakagami small-scale fading model, this paper assumes that the instantaneous value of small-scale fading between the user and its serving station is the Nakagami-m random variable. Thus, the power gain of this channel follows the normalized Gamma function with the following CDF

$$\mathbf{F}_G^{(m)}(x) = \frac{\gamma(m, mx)}{\Gamma(m)} \tag{12}$$

where $\gamma(s,x) = \int_0^x t^{s-1}e^{-t}dt$ and $\Gamma(x)$ are the incomplete and complete Gamma functions.

By substituting $u = \frac{t}{m}$, and then $t = (pu)^p$, $\mathbf{F}_G^{(m)}(x)$ is re-written as follows

$$F_G(x) = \frac{1}{\Gamma(p+1)} \int_0^{(px)^p} \exp\left(-t^{\frac{1}{p}}\right) dt \tag{13}$$

As proved from the literature [29] which states that

$$\frac{1}{\Gamma(1+1/v)} \int_0^z \exp\left(-t^v\right) dt \approx \left[1 - \exp\left(-\beta z^v\right)\right]^{1/v}$$

with $\beta = [\Gamma(1+1/v)]^{-p}$, the approximation of $F_G(x)$ is obtained as follows

$$F_G(x) \approx \left[1 - \exp\left(-\Upsilon_p x\right)\right]^p \tag{14}$$

where $\Upsilon_p = p\left[\Gamma(1+p)\right]^{-1/p}$. By utilizing the Newton's generalized binomial theorem,

$$F_S(x) \approx \sum_{m=0}^{M} \rho(p,m)(-1)^m \exp\left(-m\Upsilon_p x\right) \tag{15}$$

where $\rho(m,k) = \dfrac{m(m-1)...(m-k+1)}{k!}$; M is an integer, and selected so that the approximation converges. Particularly, a higher value of M results in a higher accuracy. In this paper, $M = 10$ is chosen to obtain a high accuracy.

In the indoor environment, the signals are usually blocked by interior walls which are randomly distributed in the service area following the Spatial PPP with density λ_w. The length of a arbitrary wall is a random variable with a mean of L where its thickness is ignored. Thus, the average number of walls on the wireless link over a distance of r is [6]:

$$W(r) = \frac{2\lambda_w L}{\pi} r = \beta r \tag{16}$$

where $\beta = \frac{2\lambda_w L}{\pi}$.

Due to the random appearance of walls, the typical user can communicate with BSs through either LoS or nLoS scenario. As computed from literature, the probability of LoS existence p_l is [30]

$$p_l(r) = \exp\left(-\beta r\right) \tag{17}$$

The probability of nLoS is $p_n(r) = 1 - p_l(r)$. With assumption that each scenario follows the conventional propagation model, the path loss model in the system is expressed as follows

$$L(r) = \begin{cases} L_l(r) = r^{-\alpha} & \text{in the case of LoS} \\ L_n(r) = \omega^{\beta r} r^{-\alpha} & \text{in the case of nLoS} \end{cases}$$

where α are the path loss coefficient; w is the path loss of a single wall. It is noted that the common model in the literature uses ζ as the path loss at the reference point which is usually at a distance of 1 m [30]. Since ζ on a given band is a constant number for all users and can be compensated by increasing the transmission power, we ignore this parameter in the path loss model.

For better expression, the path loss model is re-written as the following equation

$$L(r) = L_z(r) = \omega_z^{\beta r} r^{-\alpha} \text{ with a probability of } p_z(r) \tag{18}$$

where $z = \{n, l\}$ corresponds to LoS and nLoS, respectively; $\omega_l = 1$ and $\omega_n = \omega$.

2. Performance analysis

2.1. Relay successful decoding probability

Lemma 1. The probability that the second nearest BS of the typical user successfully decodes the received messages from the serving BS of the that user is

$$\mathcal{P}_r = \frac{1}{2}\sum_{k=1}^{M}(-1)^{k+1}\rho(m,k)\sum_{z\in\{n,l\}}\sum_{i=1}^{n^{(Le)}}\omega_i^{(Le)}\sum_{j=1}^{n^{(La)}}\omega_j^{(La)}\sum_{h=1}^{n^{(Le)}}\omega_h^{(Le)}$$
$$\frac{1-\zeta_h^{(Le)}}{2}\left[\exp\left(-\frac{k\Upsilon_m T_r}{SNR^{(br)}L_z\left(\sqrt{\frac{x_j}{\pi\lambda}}\mathcal{R}\left(\frac{1}{2}\zeta_i^{(Le)}+\frac{1}{2},\pi\zeta_h^{(Le)}+\pi\right)\right)}\right)\right]d\phi$$
$$x_j p_z\left(\sqrt{\frac{x_j}{\pi\lambda}}\mathcal{R}\left(\frac{1}{2}\zeta_i^{(Le)}+\frac{1}{2},\pi\zeta_h^{(Le)}+\pi\right)\right)$$

where $(\zeta^{(Le)}, \omega^{(Le)})$ and $(\zeta^{(La)}, \omega^{(La)})$ are the coefficients of Gauss–Legendre and Gauss - Laguerre quadratures respectively; $SNR^{(br)} = P^{(b)}/\sigma^2$. $\mathcal{R}\left(t, \phi^{(br)}\right) = \sqrt{t+1-2\sqrt{t}\cos\phi^{(br)}}$.

It is noted that the probability $\mathcal{P}_r$ also represents the probability that a relay creates interference to the typical users on the same band at the adjacent cells. The density of BSs that work as a DF relays on the same sub-band is

$$\lambda_r = \mathcal{P}_r\lambda \tag{19}$$

Proof. See Appendix E □

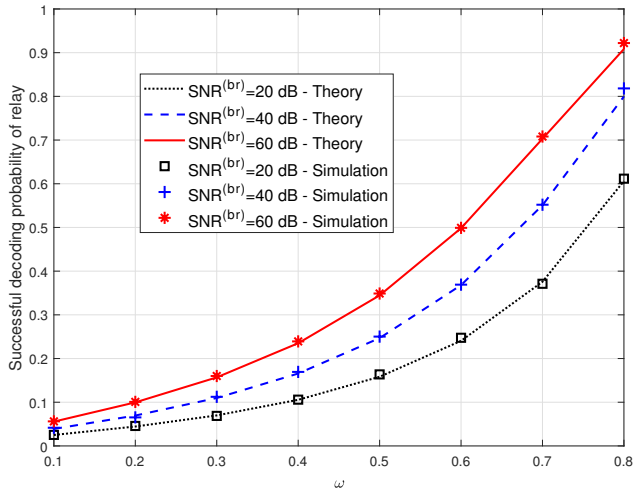

Figure 2. Successful decoding probability of relay vs transmission coefficient of each wall ω

Figure 2 illustrates that the probability that the second nearest BS of the typical user can successfully decode the received messages from its nearest BS, which is also the probability that the second nearest BS works as a relay for the typical user at adjacent cell. Due to relatively large distances between BSs, the link between these stations is usually nLoS. Thus, the path loss and consequently the received signal strength at the relay strongly depends on the density of walls and their attenuation coefficients. Particularly, a higher value of the transmission coefficient of each wall ω results in a lower path loss and a higher successful decoding probability which is shown in Figure 2. For example, when β increases by 3 times from 0.2 to 0.6, the successful decoding probability grows by 5 times from 0.1 to 0.5 in the case of $SNR = 10$ dB.

Theorem 1. The closed-form expression of Laplace transform of the interference of the typical user in the wireless transmission with LoS/nLoS model as the small-scale fading and omission of fast fading is determined by

$$\mathcal{L}(s, r^{(ru)}) = \exp\left(-2\pi\lambda_r \sum_{q=1}^{M}\binom{M}{p}(-s)^q\left[\frac{P^{(ru)}+P^{(b)}}{M}\right]^q\begin{pmatrix}\mathcal{I}_l\left(q,\omega_l,r^{(ru)}\right)\\+\mathcal{I}_n\left(q,\omega_n,r^{(ru)}\right)\end{pmatrix}\right)\exp\left(-2\pi(\lambda-\lambda_r)\sum_{q=1}^{M}\binom{M}{p}(-s)^q\left[\frac{P^{(b)}}{M}\right]^q\begin{pmatrix}\mathcal{I}_l\left(q,\omega_l,r^{(ru)}\right)\\+\mathcal{I}_n\left(q,\omega_n,r^{(ru)}\right)\end{pmatrix}\right) \tag{20}$$

where $\mathcal{I}_l\left(q,\omega_l,r^{(ru)}\right)$ and $\mathcal{I}_n\left(q,\omega_n,r^{(ru)}\right)$ are computed from Equations F.8 and F.10.

Proof. See Appendix F □

2.2. Coverage probability

As in the literature, the coverage probability of the typical user in the PPP network system with the minimum required SINR of T is defined by the following expression

$$\mathcal{P} = \mathbb{P}(SINR > T) \tag{21}$$

where $SINR$ is defined in Equation 10. Substituting the SINR's definition in Equation 10 with reminding that $\frac{S^{(ru)}+S^{(bu)}}{I+\sigma^2}$ and $SNR^{(br)}$, and $\frac{S^{(bu)}}{I+\sigma^2}$ and $SNR^{(br)}$ are pairs of independent random variables, the coverage probability is represented as

$$\begin{aligned}\mathcal{P} =&\mathbb{P}\left(\frac{S^{(ru)}+S^{(bu)}}{I+\sigma^2}>T\right)P(SNR^{(br)}>T_r)\\&+\mathbb{P}\left(\frac{S^{(bu)}}{I+\sigma^2}>T\right)P(SNR^{(br)}<T_r)\end{aligned} \tag{22}$$

where $\mathcal{P}_{wo} = \mathbb{P}\left(\frac{S^{(ru)}+S^{(bu)}}{I+\sigma^2}>T\right)$ and $\mathcal{P}_w = \mathbb{P}\left(\frac{S^{(bu)}}{I+\sigma^2}>T\right)$ are the coverage probability of the typical user if it is served by the serving BS with and without relay assistance. In the following theorems, $\mathcal{P}_{wo}$ and $\mathcal{P}_w$ are derived.

Theorem 2. The coverage probability of the typical user in the proposed system without the relay assistance is given by

$$\mathcal{P}_{wo} = \sum_{u\in\{n,l\}}\sum_{k=1}^{M}(-1)^{k+1}\rho(m,k)\int_0^\infty\int_{r^{(bu)}}^\infty\left[\begin{array}{c}\exp\left(-\frac{k\Upsilon_m T}{SNR^{(br)}\omega_u^{\beta r^{(bu)}}\left[r^{(bu)}\right]^{-\alpha}}\right)\\\mathcal{L}\left(\frac{k\Upsilon_m T}{P^{(b)}\omega_u^{\beta r^{(bu)}}\left[r^{(bu)}\right]^{-\alpha}},r^{(ru)}\right)\\p_u\left(r^{(bu)}\right)f_{12}\left(r^{(bu)},r^{(ru)}\right)\end{array}\right]dr^{(ru)}dr^{(bu)} \tag{23}$$

and its approximation is

$$\mathcal{P}_{wo} = \frac{1}{2}\sum_{u\in\{n,l\}}\sum_{k=1}^{M}(-1)^{k+1}\rho(m,k)\sum_{p=1}^{n^{(La)}}\omega_p^{(La)}\zeta_p^{(La)}\sum_{v=1}^{n^{(Le)}}w_v^{(Le)}\left[\begin{array}{c}\exp\left(-\frac{k\Upsilon_m T\tau^\alpha}{SNR^{(br)}\omega_u^{\beta\tau}}\right)\\\mathcal{L}\left(\frac{k\Upsilon_m T\tau^\alpha}{P^{(b)}\omega_u^{\beta\tau}},\sqrt{\frac{\zeta_p^{(La)}}{\pi\lambda}}\right)p_u(\tau)\end{array}\right] \tag{24}$$

where $\tau = \sqrt{\frac{\zeta_p^{(La)}}{\pi\lambda}\left(\frac{1}{2}\zeta_v^{(Le)}+\frac{1}{2}\right)}$; $\mathcal{L}(.,.)$ is defined in Equation 20.

Proof. See Appendix G □

Theorem 3. The coverage probability of the typical user with relay assistance in the proposed system is obtained by

$$\mathcal{P}_w = \sum_{u=\{n,l\}} \sum_{v=\{n,l\}} \sum_{k=0}^{M} \rho(m,k)(-1)^k \int_0^{\infty} \int_0^{r^{(ru)}} \left[\exp\left(-\frac{k\Upsilon_p}{y} T\sigma^2\right) \mathcal{L}\left(-\frac{k\Upsilon_p}{y} T, r^{(ru)}\right) p_u\left(r^{(bu)}\right) p_v\left(r^{(ru)}\right) f_{12}\left(r^{(bu)}, r^{(ru)}\right) \right] dr^{(bu)} dr^{(ru)} \tag{25}$$

and its approximation is

$$\mathcal{P}_{wo} = \frac{1}{2} \sum_{u\in\{n,l\}} \sum_{v=\{n,l\}} \sum_{k=1}^{M} \sum_{p=1}^{n^{(La)}} \sum_{v=1}^{n^{(Le)}} \left[(-1)^{k+1} \rho(m,k) \omega_p^{(La)} \zeta_p^{(La)} w_v^{(Le)} \exp\left(-\frac{k\Upsilon_p}{y} T\sigma^2\right) \mathcal{L}\left(\frac{k\Upsilon_p}{y} T, \sqrt{\frac{\zeta_p^{(La)}}{\pi\lambda}}\right) p_u(\tau)\, p_v\left(\sqrt{\frac{\zeta_p^{(La)}}{\pi\lambda}}\right) \right]$$

where $p = \frac{m\left[P^{(b)}\omega_u^{\beta\tau} t^{-\alpha/2} + P^{(r)}\omega_v^{\beta r}\right]^2}{\left[P^{(b)}\omega_u^{\beta\tau} t^{-\alpha/2}\right]^2 + \left[P^{(r)}\omega_v^{\beta r}\right]^2}$; $y = \left[P^{(b)} L_u(\tau) + P^{(r)} L_v(r)\right]$; $\Upsilon_p = [\Gamma(1+p)]^{-1/p}$ $\tau = \sqrt{\frac{\zeta_p^{(La)}}{\pi\lambda}\left(\frac{1}{2}\zeta_v^{(Le)} + \frac{1}{2}\right)}$; $t = \sqrt{\frac{1}{2}\zeta_v^{(Le)} + \frac{1}{2}}$; and $r = \sqrt{\frac{\zeta_p^{(La)}}{\pi\lambda}}$; $\mathcal{L}(.,.)$ is defined in Equation 20.

Proof. See Appendix H □

3. Simulation and Discussion

3.1. Theoretical Validation

In this section, we adopt different values of the coverage threshold T and density of BSs λ to compute the coverage probability of the typical user with and without relay assistance by following both theoretical results of Theorems 2 and 3 and Monte Carlo simulation. The adopted parameters are summarized as follows:

- The density of walls is $\lambda_w = 0.1$ $(wall/m^2)$ where their average length is 3.5 m;
- The transmission coefficient of each wall is $\omega = 0.8$.
- The probability that a BS acts as a relay for the typical user at adjacent cell is 90%.
- The standard transmission power of the BS to the its associated user is 30 dB higher than the Gaussian noise power. Meanwhile the BS utilizes 2 dB less than the standard transmission power when it acts as a relay.

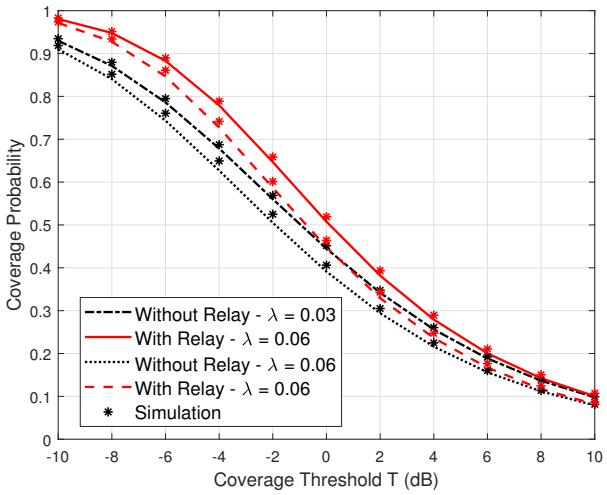

Figure 3. Coverage Probability vs Coverage Threshold

As demonstrated from Figure 3, the analytical and simulation results are the same for all the examined cases of coverage threshold T, and density of BSs λ. This match confirms the accuracy of Theorems 2 and 3.

The figure also shows that the both user with and without relay assistance experience a downtrend of coverage probabilities when coverage threshold T increases. For example, when T increases by 2 dB, the coverage probability of the typical user with relay assistance in the network with $\lambda = 0.06$ (BS/m^2) reduces by 13.9% from 0.9 to 0.79. This is reasonable due to the coverage threshold indicates the decoding ability of the end devices. A higher value of T reflects a higher required signal quality and a lower coverage probability. Furthermore, it is seen that for all values of T, the coverage probability of the typical user with relay assistance is higher than another without relay assistance. Take $\lambda = 0.03$ and $T = -8$ dB for example, the coverage probability of the typical user with relay assistance is nearly 0.95 which is 6.7% higher than that of another user. This improvement in the user coverage probability is due to the desired signal power improvement of the proposed system. In the next sections, the benefits of the proposed system will be highlighted in more detail.

3.2. Effects of density of walls on user performance

In this section, the coverage probability of the typical user in the proposed system is compared with another in the conventional system. In the proposed system, besides signal from the serving BS $S^{(bu)}$, the typical user can be served with additional assistance from the second nearest BS $S^{(ru)}$ but it also suffers interference from each BS twice: *(i)* the first time when the BS serves its associated user. The total interference is I_f, *(ii)* the second time when the BS works as a relay

to assist the typical user at the adjacent cell. The total interference in this case is I_f while the typical user in the conventional system is only served by its nearest BS with the desired signal power of $S^{(ru)}$ and affected by interference from others once and the total interference is I_f. The following equations compare the downlink SINR of the typical user in the proposed and conventional system models

$$SINR_{pro} = \frac{S^{(ru)} + S^{(bu)}}{I_f + I_s + \sigma^2} \quad \text{and} \quad SINR_{conv} = \frac{S^{(bu)}}{I_s + \sigma^2} \tag{26}$$

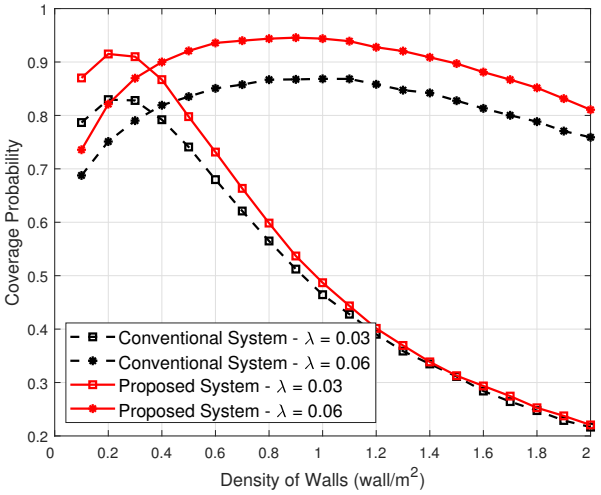

Figure 4. Effects of density of walls on the typical user performance

Although the typical user in the proposed system suffers a higher interference level than another in the conventional one, it can achieve a higher coverage probability. For example, when the density of walls is 0.6 $(wall/m^2)$ or 1 $wall/3m^2$ which can be found in the indoor closed-office environment, the coverage probability of the typical user in the proposed system is 0.94 which is 10.5% higher than that of the typical user in the conventional one that has the same density of BSs of 0.06 (BS/m^2). This increase in the user coverage probability proves that the benefits of the desired signal power improvement from $S^{(ru)}$ to $S^{(ru)} + S^{(bu)}$ in the proposed system model can overcome the increment of intercell interference. However, there is a slight improvement in the coverage probability of the typical user in the proposed and conventional ones when the density of walls $\lambda_w > 1$ $(wall/m^2)$ and $\lambda = 0.03$ as illustrated in Figure 4. This may be the result of the balance between the increase in the desired signal and interference power. Consequently, it can be concluded that the proposed system model can provide an improvement in the coverage probability of the typical user at a maximum of 10% when $\lambda = 0.06$.

An interesting fact can be seen from the Figure 4 that the coverage probability increases to the peaks of such as 0.91 in the proposed system model and 0.87 in the conventional system model with $\lambda = 0.03$ (BS/m^2), before passing a slow and fast decline in the case of $\lambda = 0.03$ (BS/m^2) and $\lambda = 0.06$ (BS/m^2) respectively. This performance trend is the result of the following aspects:

- The probability that the signal from the BSs to the typical user is blocked is proportional to the density of walls. In other words, the probability of nLoS and then the path loss increases with the density of walls λ_w. Thus, when λ_w increases both the desired and interference signal powers of the typical user in both systems increase.
- When λ_w increases, and $\lambda_w < 0.2(wall/m^2)$ in the case of $\lambda = 0.03$ (BS/m^2) and $\lambda_w < 0.8$ $(wall/m^2)$ in the case of $\lambda = 0.06$ (BS/m^2), the desired signal still obtains the LoS with a high probability while the interference signals are usually nLoS. Thus, the desired signal power of the typical user declines at a lower rate than the interference power does. Thus, the coverage probability increases. Take the proposed system with $\lambda = 0.03$ for example, when λ_w grows from 0.1 to 0.2, the coverage probability increases and reaches the peak of 0.92
- When λ_w increases, and $\lambda_w > 0.2$ and $\lambda_w > 0.8$ in the cases of $\lambda = 0.03$ and $\lambda = 0.06$ (BS/m^2) respectively, the desired and interference signals are likely blocked by the walls. Thus, the decline rate of the desired signal is higher than that of the interference signals. Consequently, the coverage probability reduces.

3.3. Effects of density of BSs on the typical user performance

The relationship between the user coverage probability and the density of BSs with different value of transmission property of walls $\omega = 0.4, 0.8$ is visualized in Figure 5. Since the B5G and 6G networks are expected to serve the massive connectivity which maybe upto 10^7 devices in every km^2 [31]. Thus, Figure 5 examines the user performance when density of BSs λ varies from 0.01 to 0.1 BS/m^2, i.e. $10^4 - 10^5$ BS/km^2.

In the case of $\omega = 0.4$, the power that passes through the wall over a distance of d is $0.4^d << 1$ which means that most of the signal's power is lost as it travels through walls. While the link between the serving BS and the relay is usually nLoS which is blocked by walls, the relay is possibly unable to decode the messages from the serving BS. Thus, the typical user is only served by the nearest BS. As a result, the coverage probability of the typical user in the proposed system

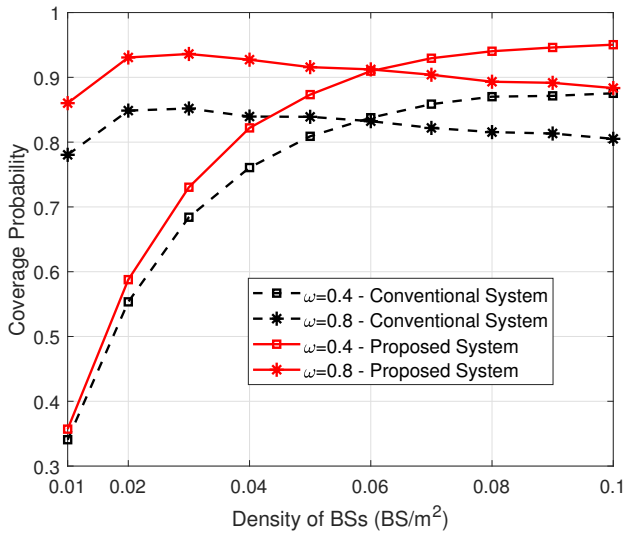

Figure 5. Effects of density of BSs on the typical user performance

is similar to another in the conventional one. When the density of BSs λ increases, the serving BS is closer than the relay. Thus, the received signal strength and consequently the successful decoding probability of the relay increases. In other words, the probability that a typical user is served by both the serving BS and relay increases with the density of BSs λ. Hence, the user coverage probability, and then the gap between the coverage probability in the proposed and conventional systems increase with λ. As seen from Figure 5, when λ increases from 0.01 (BS/m^2) to 0.1 (BS/m^2), the user coverage probability in the proposed system rises by 163% from 0.36 to 0.95, and is 8% higher than another in the conventional system.

In the case of $\omega = 0.8$, most of signal power passes through the walls. Thus, the relay can successfully decode the received messages from the serving BS with a high probability. In other words, the communication between the typical user and its serving BS in this case is usually assisted by the relay. Consequently, the typical user in the proposed system achieves a significantly higher coverage probability than another in the conventional one for different values of density of BSs λ in the case of $\omega = 0.8$ as seen from this figure. For example, when $\lambda = 0.04$ (BS/m^2) and $\omega = 0.8$, the typical user in the proposed system can have a coverage probability of 0.93 which is 10.7% higher than another in the conventional system.

It also seen from the figure that the coverage probability of the typical user reduces in the case of $\omega = 0.8$ $(wall/m^2)$ but increases in the case of $\omega = 0.4$ $(wall/m^2)$ as λ increase. These results refer to the increasing trend of both desired and interference signal powers when the network becomes denser. Since the distances between the typical user and other BSs shrink as λ increases, the power of signals at the typical user, including desired signal and interfering signals, increases. In the case of $\omega = 0.8$, the interfering signal power increases than the desired signal. Thus, the coverage probability reduces. Meanwhile, in the case of $\omega = 0.4$, almost the power of the interfering signals is lost due to the walls, the desired signal goes up at a higher rate than that of interfering signals as λ grows. Thus, the coverage probability increases in this case.

4. Conclusion

In this paper, the new cooperative communication paradigm was introduced to allow the typical to be served by both the nearest and second nearest BS where the former is the primary serving BS, and the latter works as the DF relay. In particular, the second nearest BS only works as the relay for the typical user if it successfully decodes the message from the serving BS. Thus, the power-domain NOMA technique is applied to allow the relay to transmit on the same frequency band with the serving BS but at lower transmission power. The coverage probability expressions and their closed-form expression of the typical user with and without relay assistance in the proposed system are derived in the wireless environment with Nakagami-m as small-scale fading and the newly developed path loss model, that examines the effects of density of walls and their properties, as the large-scale fading. The analytical results illustrate that the typical user in the proposed system can achieve a higher coverage probability than another in the conventional system in all cases of density of walls and density of BSs.

E. Appendix

The probability, that the BS can successfully decode the message from the serving BS of the typical user to work as a relay, is defined in Equation 6.

$$\mathcal{P}_r = \mathbb{P}\left(SNR^{(br)} > T_r\right) \tag{E.1}$$

Substituting the definition of $SNR^{(br)}$ in Equation 5b with reminding that $L(r)$ is combination of two independent events, e.g. LoS and nLoS, as described in 18, into this equation, we obtain

$$\begin{aligned}\mathcal{P}_r &= \sum_{z\in\{n,l\}} \mathbb{E}\left[\mathbb{P}\left(\frac{P^{(b)} g_z^{(b)} L_z\left(r^{(br)}\right)}{\sigma^2} > T_r\right) p_z\left(r^{(br)}\right) \middle| \left(r^{(br)}\right)\right] \\ &= \sum_{z\in\{n,l\}} \mathbb{E}\left[\mathbb{P}\left(g_z^{(b)} > \frac{T_r}{SNR^{(b)} L_z\left(r^{(br)}\right)}\right) p_z\left(r^{(br)}\right) \middle| \left(r^{(br)}\right)\right]\end{aligned}$$

Substituting the approximation form of CDF in Equation 15, $\mathcal{P}_r$ is obtained by

$$\mathcal{P}_r = \sum_{k=1}^{M}(-1)^{k+1}\rho(m,k)\sum_{z\in\{n,l\}} \mathbb{E}\left[\exp\left(-\frac{k\Upsilon_m T_r}{SNR^{(br)}L_z\left(r^{(br)}\right)}\right)p_z\left(r^{(br)}\right)\middle|\left(r^{(br)}\right)\right] \quad \text{(E.2)}$$

where $r^{(br)}$ is the function of ϕ, $r^{(bu)}$ and $r^{(ru)}$ as in Equation 2.

Therefore, evaluating the expectation with respects to ϕ, $r^{(bu)}$ and $r^{(ru)}$, the successfully decoding probability $\mathcal{P}_r$ is given by

$$\mathcal{P}_r = \sum_{k=1}^{M}(-1)^{k+1}\rho(m,k)\int_0^{\infty}\int_{r^{(bu)}}^{\infty}\int_0^{2\pi} \sum_{z\in\{n,l\}}\begin{bmatrix}\exp\left(-\frac{k\Upsilon_m T_r}{SNR^{(br)}L_z\left(r^{(br)}\right)}\right)\\ p_z\left(r^{(br)}\right)f_{12}\left(r^{(bu)},r^{(ru)}\right)f_\Phi(\phi)\end{bmatrix}d\phi dr^{(ru)}dr^{(bu)}$$

where $f_{12}\left(r^{(bu)},r^{(ru)}\right)$ and $f_\Phi(\phi)$ are defined in Equations 1 and 3. Substituting the join PDF of $r^{(bu)}$ and $r^{(ru)}$, and $p_z\left(r^{(br)}\right)$ we obtain

$$\mathcal{P}_r = \sum_{k=1}^{M}(-1)^{k+1}\rho(m,k)\sum_{z\in\{n,l\}}\int_0^{2\pi}\int_0^{\infty}\int_0^{r^{(ru)}} \begin{bmatrix}\exp\left(-\frac{k\Upsilon_m T_r}{SNR^{(br)}L_z\left(r^{(br)}\right)}\right)p_z\left(r^{(br)}\right)\\ (2\pi\lambda)^2 r^{(bu)}r^{(ru)}\exp\left(-\pi\lambda\left[r^{(ru)}\right]^2\right)f_\Phi(\phi)\end{bmatrix}dr^{(bu)}dr^{(ru)}d\phi$$

Employing a change of variable $x = r^{(bu)}/r^{(ru)}$ which is followed by $t = x^2$, then $r^{(br)} = r^{(ru)}\sqrt{t+1-2\sqrt{t}\cos\phi^{(br)}} = r^{(ru)}\mathcal{R}\left(t,\phi^{(br)}\right)$, and

$$\mathcal{P}_r = \frac{1}{2}\sum_{k=1}^{M}(-1)^{k+1}\rho(m,k)\int_0^{2\pi}f_\Phi(\phi)\int_0^{\infty} \begin{bmatrix}\left[(2\pi\lambda)^2 r^{(ru)}\right]^2\exp\left(-\pi\lambda\left[r^{(ru)}\right]^2\right)\\ \sum_{z\in\{n,l\}}\int_0^1\exp\left(-\frac{k\Upsilon_m T_r}{SNR^{(br)}L_z\left(r^{(ru)}\mathcal{R}\left(t,\phi^{(br)}\right)\right)}\right)\\ p_z\left(r^{(ru)}\mathcal{R}\left(t,\phi^{(br)}\right)\right)dt\end{bmatrix}dr^{(ru)}d\phi$$

Since finding the closed-form expression of this coverage probability expression is a big challenge, this paper aims to find its approximation form. The inner integral can be approximated by the Gauss–Legendre quadrature which states that $\int_a^b f(x)dx = \frac{(b-a)}{2}\sum_{i=1}^{n^{(Le)}} w_i^{(Le)} f\left(\frac{b-a}{2}\zeta_i^{(Le)} + \frac{a+b}{2}\right)$, then

$$\mathcal{P}_r = \sum_{k=1}^{M}(-1)^{k+1}\rho(m,k)\sum_{z\in\{n,l\}}\sum_{i=1}^{n^{(Le)}} w_i^{(Le)} \int_0^{2\pi}f_\Phi(\phi)\int_0^{\infty} \begin{bmatrix}(\pi\lambda)^2\left[r^{(ru)}\right]^3\exp\left(-\pi\lambda\left[r^{(ru)}\right]^2\right)\\ \exp\left(-\frac{k\Upsilon_m T_r}{SNR^{(br)}L_z\left(r^{(ru)}\mathcal{R}\left(\frac{1}{2}\zeta_i^{(Le)}+\frac{1}{2},\phi^{(br)}\right)\right)}\right)\\ p_z\left(r^{(ru)}\mathcal{R}\left(\frac{1}{2}\zeta_i^{(Le)}+\frac{1}{2},\phi^{(br)}\right)\right)\end{bmatrix}dr^{(ru)}d\phi$$

By changing of the variable of $y = \pi\lambda\left[r^{(ru)}\right]^2$, then $r^{(ru)} = \sqrt{\frac{y}{\pi\lambda}}$. Thus, $\mathcal{P}_r$ becomes

$$\mathcal{P}_r = \frac{1}{2}\sum_{k=1}^{M}(-1)^{k+1}\rho(m,k)\sum_{z\in\{n,l\}}\sum_{i=1}^{n^{(Le)}} w_i^{(Le)} \int_0^{2\pi}f_\Phi(\phi)\int_0^{\infty} \begin{bmatrix}\exp\left(-\frac{k\Upsilon_m T_r}{SNR^{(br)}L_z\left(\sqrt{\frac{y}{\pi\lambda}}\mathcal{R}\left(\frac{1}{2}\zeta_i^{(Le)}+\frac{1}{2},\phi^{(br)}\right)\right)}\right)\\ y\exp(-y)\,p_z\left(\sqrt{\frac{y}{\pi\lambda}}\mathcal{R}\left(\frac{1}{2}\zeta_i^{(Le)}+\frac{1}{2},\phi^{(br)}\right)\right)\end{bmatrix}dyd\phi$$

The inner integral has a form of Gauss–Laguerre quadrature which concludes that $\int_0^{\infty}e^{-x}f(x)dx = \sum_{j=1}^{n^{(La)}}\omega_j^{(La)}f(x_j)$, then it can be approximated by

$$\mathcal{P}_r = \frac{1}{2}\sum_{k=1}^{M}(-1)^{k+1}\rho(m,k)\sum_{z\in\{n,l\}}\sum_{i=1}^{n^{(Le)}} w_i^{(Le)}\sum_{j=1}^{n^{(La)}}\omega_j^{(La)} \int_0^{2\pi}f_\Phi(\phi)\begin{bmatrix}\exp\left(-\frac{k\Upsilon_m T_r}{SNR^{(br)}L_z\left(\sqrt{\frac{x_j}{\pi\lambda}}\mathcal{R}\left(\frac{1}{2}\zeta_i^{(Le)}+\frac{1}{2},\phi^{(br)}\right)\right)}\right)\\ x_j p_z\left(\sqrt{\frac{x_j}{\pi\lambda}}\mathcal{R}\left(\frac{1}{2}\zeta_i^{(Le)}+\frac{1}{2},\phi^{(br)}\right)\right)\end{bmatrix}d\phi$$

The integral has a suitable form of Gauss–Legendre quadrature. Thus the coverage probability is finally approximated by

$$\mathcal{P}_r = \frac{1}{2}\sum_{k=1}^{M}(-1)^{k+1}\rho(m,k)\sum_{z\in\{n,l\}}\sum_{i=1}^{n^{(Le)}} w_i^{(Le)}\sum_{j=1}^{n^{(La)}}\omega_j^{(La)}\sum_{h=1}^{n^{(Le)}} w_h^{(Le)} \frac{1-\zeta_h^{(Le)}}{2}\begin{bmatrix}\exp\left(-\frac{k\Upsilon_m T_r}{SNR^{(br)}L_z\left(\sqrt{\frac{x_j}{\pi\lambda}}\mathcal{R}\left(\frac{1}{2}\zeta_i^{(Le)}+\frac{1}{2},\pi\zeta_h^{(Le)}+\pi\right)\right)}\right)\\ x_j p_z\left(\sqrt{\frac{x_j}{\pi\lambda}}\mathcal{R}\left(\frac{1}{2}\zeta_i^{(Le)}+\frac{1}{2},\pi\zeta_h^{(Le)}+\pi\right)\right)\end{bmatrix}d\phi$$

F. Appendix

Under the LoS and nLoS scenarios, the total interference in Equation 11 is expanded as follows

$$\begin{aligned} I &= \sum_{k\in\theta^{(r)}} P^{(ru)} L(r_k^{(ru)}) + \sum_{h\in\theta^{(b)}} P^{(b)} L(r_h^{(bu)}) \\ &= \sum_{k\in\theta^{(r)}} \left[P^{(ru)} + P^{(b)}\right] L(r_k^{(ru)}) + \sum_{h\in\theta^{(b)}\setminus\theta^{(r)}} P^{(b)} L(r_h^{(bu)}) \\ &= \sum_{z\in\{n,l\}} \sum_{k\in\theta^{(zr)}} \left[P^{(ru)} + P^{(b)}\right] L_z(r_k^{(ru)}) \\ &\quad + \sum_{z\in\{n,l\}} \sum_{h\in\theta^{(zb)}\setminus\theta^{(r)}} P^{(b)} L_z(r_h^{(bu)}) \end{aligned} \tag{F.3}$$

where $\theta^{(zr)}$ and $\theta^{(zb)}$, where $z = \{n, l\}$, is the set of interfering relays and BSs of the typical user via the z links, respectively; $\theta^{(lr)} \cup \theta^{(nr)} = \theta^{(r)}$; and $\theta^{(br)} \cup \theta^{(br)} = \theta^{(r)}$.

Substituting the above expanded expression of I and the path loss definition in Equation 18 into to its Laplace transform which is defined by $\mathcal{L}(s, r^{(ru)}) = \mathbb{E}\left[\exp\left(-sI\right)\right]$, we obtain $\mathcal{L}(s, r^{(ru)}) =$

$$\begin{aligned} &\mathbb{E}\left[\prod_{z\in\{n,l\}} \prod_{k\in\theta^{(zr)}} \exp\left(-s\left[P^{(ru)} + P^{(b)}\right] \omega_z^{\beta r_k^{(ru)}} \left[r_k^{(ru)}\right]^{-\alpha}\right)\right] \\ &\mathbb{E}\left[\prod_{z\in\{n,l\}} \prod_{h\in\theta^{(zb)}\setminus\theta^{(r)}} \exp\left(-sP^{(b)} \omega_z^{\beta r_k^{(ru)}} \left[r_h^{(bu)}\right]^{-\alpha}\right)\right] \end{aligned} \tag{F.4}$$

Since $0 < \omega_z \leq 1$ and $r_k^{(ru)} > 1(m)$, $\omega_z^{\beta r_k^{(ru)}} < 1$ and $\left[r_k^{(ru)}\right]^{-\alpha} < 1$. Therefore, if $s\left[P^{(ru)} + P^{(b)}\right] < M$ where M is an integer, $\frac{1}{M}\omega_z^{\beta r_k^{(ru)}} \left[r_k^{(ru)}\right]^{-\alpha} << 1$ and $\frac{1}{M} sP^{(b)} \omega_z^{\beta r_k^{(ru)}} \left[r_h^{(bu)}\right]^{-\alpha} << 1$. Employing the Taylor expansion consequence which states that $\exp(-x) \approx 1 - x$ for $0 < x << 1$, $\mathcal{L}(s, r^{(ru)})$ approximates to $\mathcal{L}(s, r^{(ru)}) =$

$$\begin{aligned} &\mathbb{E}\left[\prod_{z\in\{n,l\}} \prod_{k\in\theta^{(zr)}} \left(1 - \frac{s\left[P^{(ru)} + P^{(b)}\right]}{M} \omega_z^{\beta r_k^{(ru)}} \left[r_k^{(ru)}\right]^{-\alpha}\right)^M\right] \\ &\mathbb{E}\left[\prod_{z\in\{n,l\}} \prod_{h\in\theta^{(zb)}\setminus\theta^{(r)}} \left(1 - \frac{sP^{(b)}}{M} \omega_z^{\beta r_k^{(ru)}} \left[r_h^{(bu)}\right]^{-\alpha}\right)^M\right] \\ =&\mathbb{E}\left[\prod_{z\in\{n,l\}} \prod_{k\in\theta^{(zr)}} \sum_{q=0}^{M} \binom{M}{q} (-s)^q \left[\frac{P^{(ru)} + P^{(b)}}{M}\right]^q \omega_z^{q\beta r_k^{(ru)}} \left[r_k^{(ru)}\right]^{-q\alpha}\right] \\ &\mathbb{E}\left[\prod_{z\in\{n,l\}} \prod_{h\in\theta^{(zb)}\setminus\theta^{(r)}} \sum_{q=0}^{M} \binom{M}{q} (-s)^q \left[\frac{P^{(b)}}{M}\right]^q \omega_z^{q\beta r_k^{(ru)}} \left[r_h^{(bu)}\right]^{-q\alpha}\right] \end{aligned} \tag{F.5}$$

By following the Moment Generating Function properties, we obtain $\mathcal{L}(s, r^{(ru)}) =$

$$\begin{aligned} &\prod_{z\in\{n,l\}} \exp\left(\frac{2\pi\lambda_r \sum_{q=1}^{M} \binom{M}{q} (-s)^q \left[\frac{P^{(ru)}+P^{(b)}}{M}\right]^q}{\int_{r^{(ru)}}^{\infty} \omega_z^{q\beta r^{(ru)}} \left[r^{(ru)}\right]^{1-q\alpha} p_z\left[r^{(ru)}\right] dr^{(ru)}}\right) \\ &\prod_{z\in\{n,l\}} \exp\left(\frac{2\pi(\lambda-\lambda_r) \sum_{q=1}^{M} \binom{M}{q} (-s)^q \left[\frac{P^{(b)}}{M}\right]^q}{\int_{r^{(ru)}}^{\infty} \omega_z^{q\beta r^{(bu)}} \left[r^{(bu)}\right]^{1-q\alpha} p_z\left(r^{(bu)}\right) dr^{(bu)}}\right) \end{aligned} \tag{F.6}$$

Considering first part of Equation F.6 with $z = l$. Letting the integral of the first part with $z = l$ in the above equation $\int_{r^{(ru)}}^{\infty} \omega_z^{q\beta r^{(ru)}} \left[r^{(ru)}\right]^{1-q\alpha} p_z\left[r^{(ru)}\right] dr^{(ru)} = \mathcal{I}_l(n)$ and changing of variable $y = -(q \ln \omega_l - 1)\beta r_k^{(ru)}$, then $\mathcal{I}_z(n)$ is evaluated by the following step

$$\begin{aligned} &\mathcal{I}_l\left(q, \omega_l, r^{(ru)}\right) \\ &= \int_{(1-q\ln\omega_l)\beta r^{(ru)}}^{\infty} \left(\frac{y}{(1-q\ln\omega_l)\beta}\right)^{1-q\alpha} \frac{\exp(-y)}{(1-q\ln\omega_l)\beta} dy \\ &= \left(\frac{1}{(1-q\ln\omega_l)\beta}\right)^{2-q\alpha} \int_{(1-q\ln\omega_l)\beta r^{(ru)}}^{\infty} y^{1-q\alpha} \exp(-y) dy \end{aligned} \tag{F.7}$$

Utilize the result in [32, p.346] which concludes that $\int_u^{\infty} \frac{e^{-x}}{x^v} dx = u^{-v/2} e^{-u/2} \mathbf{W}_{-v/2,(1-v)/2}(u)$, the closed-expression of $\mathcal{I}_l\left(q, \omega_l, r^{(ru)}\right)$ is

$$\begin{aligned} &\mathcal{I}_l\left(q, \omega_l, r^{(ru)}\right) = \\ &\left((1-q\ln\omega_l)\beta\right)^{\frac{q\alpha-3}{2}} \left[r^{(ru)}\right]^{\frac{1}{2}-\frac{q\alpha}{2}} \exp\left(\frac{q\ln\omega_l - 1}{2}\beta r^{(ru)}\right) \\ &\mathbf{W}_{\frac{1-q\alpha}{2},\frac{2-q\alpha}{2}}\left((1-q\ln\omega_l)\beta r^{(ru)}\right) \end{aligned} \tag{F.8}$$

where $\mathbf{W}_{u,v}(z)$ is the Whittaker function.

Considering first part of Equation F.6 with $z = n$. By replacing the $p_z\left(r^{(bu)}\right) = 1 - \exp\left(-\beta r^{(bu)}\right)$ and $\omega_n = 1$, the integral becomes

$$\begin{aligned} &\mathcal{I}_n\left(q, \omega_n, r^{(ru)}\right) \\ &= \int_{r^{(ru)}}^{\infty} \omega_n^{q\beta r^{(bu)}} \left[r^{(bu)}\right]^{1-q\alpha} \left[1 - \exp\left(r^{(bu)}\right)\right] dr^{(bu)} \\ &= \int_{r^{(ru)}}^{\infty} \omega_n^{q\beta r^{(bu)}} \left[r^{(bu)}\right]^{1-q\alpha} dr^{(bu)} \\ &\quad - \int_{r^{(ru)}}^{\infty} \omega_n^{q\beta r^{(bu)}} \left[r^{(bu)}\right]^{1-q\alpha} \exp\left(-\beta r^{(bu)}\right) dr^{(bu)} \end{aligned} \tag{F.9}$$

The first integral is the special case of the $\omega_n = \omega_l$ and without the LoS probability element $\exp\left(-\beta r^{(bu)}\right)$. Meanwhile, the second integral is obtained by substituting ω_l by ω_n. Hence, $\mathcal{I}_n\left(q, \omega_n, r^{(ru)}\right)$ is obtained by

$$\mathcal{I}_n\left(q,\omega_n,r^{(ru)}\right) = \left(-q\ln\omega_n\beta\right)^{\frac{qa-3}{2}}\left[r^{(ru)}\right]^{\frac{1}{2}-\frac{qa}{2}}\exp\left(\frac{q\ln\omega_n}{2}\beta r^{(ru)}\right) \mathbf{W}_{\frac{1-qa}{2},\frac{2-qa}{2}}\left(-q\ln\omega_n\beta r^{(ru)}\right) - \mathcal{I}_n\left(q,\omega_n,r^{(ru)}\right) \quad \text{(F.10)}$$

The integral of second part of Equation F.6 has the same value as the integral of the first part. Consequently, the Laplace transform of interference is computed as Theorem 1.

G. Appendix

The coverage probability in this case is obtained by

$$\mathcal{P}_{wo} = \mathbb{P}\left(\frac{S^{(bu)}}{I+\sigma^2} > T\right) \quad \text{(G.11)}$$

where $S^{(bu)}$ is defined in Equation 4. Hence,

$$\mathcal{P}_{wo} = \mathbb{P}\left(\frac{P^{(b)}g^{(bu)}L\left(r^{(bu)}\right)}{I+\sigma^2} > T\right) \quad \text{(G.12)}$$

Since link between the typical user and the nearest BS at a distance of $r^{(bu)}$ is either LoS with a probability of $p_l\left(r^{(bu)}\right)$ or nLoS with a probability of $p_r\left(r^{(bu)}\right)$, $\mathcal{P}_{wo}$ is expanded as follows

$$\begin{aligned}\mathcal{P}_{wo} &= \sum_{u\in\{n,l\}}\mathbb{P}\left(\frac{P^{(b)}g_u^{(bu)}\omega_u^{\beta r^{(bu)}}\left[r^{(bu)}\right]^{-\alpha}}{I+\sigma^2} > T\right)p_u\left(r^{(bu)}\right)\\ &= \sum_{u\in\{n,l\}}\mathbb{P}\left(g_u^{(bu)} > \frac{I+\sigma^2}{P^{(b)}\omega_u^{\beta r^{(bu)}}\left[r^{(bu)}\right]^{-\alpha}}T\right)p_u\left(r^{(bu)}\right)\end{aligned} \quad \text{(G.13)}$$

Since $g_u^{(bu)}$ is a normalized Gamma random variable with the approximated CDF as in Equation **??**, the coverage probability is equal to

$$\mathcal{P}_{wo} = \sum_{u\in\{n,l\}}\sum_{k=1}^{M}(-1)^{k+1}\rho(m,k) \mathbb{E}\left[\begin{array}{c}\exp\left(-\frac{k\Upsilon_m T}{SNR^{(br)}\omega_u^{\beta r^{(bu)}}\left[r^{(bu)}\right]^{-\alpha}}\right)\\ \mathcal{L}\left(\frac{k\Upsilon_m T}{P^{(b)}\omega_u^{\beta r^{(bu)}}\left[r^{(bu)}\right]^{-\alpha}}, r^{(ru)}\right)\end{array}\right]p_u\left(r^{(bu)}\right)$$

Evaluating the expectation with respect to $r^{(bu)}$ and $r^{(ru)}$ whose PDFs are given in Equation 1, we obtain the coverage probability of the typical without relay assistance as the following equation

$$\mathcal{P}_{wo} = \sum_{u\in\{n,l\}}\sum_{k=1}^{M}(-1)^{k+1}\rho(m,k) \int_0^\infty\int_0^{r^{(ru)}}\left[\begin{array}{c}\exp\left(-\frac{k\Upsilon_m T}{SNR^{(br)}\omega_u^{\beta r^{(bu)}}\left[r^{(bu)}\right]^{-\alpha}}\right)\\ \mathcal{L}\left(\frac{k\Upsilon_m T}{P^{(b)}\omega_u^{\beta r^{(bu)}}\left[r^{(bu)}\right]^{-\alpha}}, r^{(ru)}\right)\\ p_u\left(r^{(bu)}\right)f_{12}\left(r^{(bu)}, r^{(ru)}\right)\end{array}\right]dr^{(bu)}dr^{(ru)}$$

Letting $x = r^{(bu)}/r^{(ru)}$ which is followed by $t = x^2$, we obtain

$$\begin{aligned}&\mathcal{P}_{wo}\\ &= \sum_{u\in\{n,l\}}\sum_{k=1}^{M}(-1)^{k+1}\rho(m,k)\\ &\int_0^\infty 2(\pi\lambda)^2\left[r^{(ru)}\right]^3\exp\left(-\pi\lambda\left[r^{(ru)}\right]^2\right)\\ &\left[\int_0^1\left[\begin{array}{c}\exp\left(-\frac{k\Upsilon_m T t^{\alpha/2}}{SNR^{(br)}\omega_u^{\beta r^{(ru)}\sqrt{t}}\left[r^{(ru)}\right]^{-\alpha}}\right)\\ \mathcal{L}\left(\frac{k\Upsilon_m T t^{\alpha/2}}{P^{(b)}\omega_u^{\beta r^{(ru)}\sqrt{t}}\left[r^{(ru)}\right]^{-\alpha}}, r^{(ru)}\right)\end{array}\right]p_u\left(r^{(ru)}\sqrt{t}\right)dt\right]dr^{(ru)}\end{aligned}$$

The inner integral is approximated by the Gauss–Legendre quadrature. Hence,

$$\begin{aligned}&\mathcal{P}_{wo} = \sum_{u\in\{n,l\}}\sum_{k=1}^{M}(-1)^{k+1}\rho(m,k)\\ &\int_0^\infty(\pi\lambda)^2\left[r^{(ru)}\right]^3\exp\left(-\pi\lambda\left[r^{(ru)}\right]^2\right)\\ &\left[\begin{array}{c}\sum_{i=1}^{n^{(Le)}}w_i^{(Le)}\exp\left(-\frac{k\Upsilon_m T\left[r^{(ru)}\sqrt{\frac{1}{2}\zeta_i^{(Le)}+\frac{1}{2}}\right]^\alpha}{SNR^{(br)}\omega_u^{\beta r^{(ru)}\sqrt{\frac{1}{2}\zeta_i^{(Le)}+\frac{1}{2}}}}\right)\\ \mathcal{L}\left(\frac{k\Upsilon_m T\left[r^{(ru)}\sqrt{\frac{1}{2}\zeta_i^{(Le)}+\frac{1}{2}}\right]^\alpha}{P^{(b)}\omega_u^{\beta r^{(ru)}\sqrt{\frac{1}{2}\zeta_i^{(Le)}+\frac{1}{2}}}}, r^{(ru)}\right)p_u\left(r^{(ru)}\sqrt{\frac{1}{2}\zeta_i^{(Le)}+\frac{1}{2}}\right)\end{array}\right]dr^{(ru)}\end{aligned}$$

By employing a change of variable $y = \pi\lambda\left[r^{(ru)}\right]^2$, $\mathcal{P}_{wo}$ becomes

$$\begin{aligned}&\mathcal{P}_{wo} = \frac{1}{2}\sum_{u\in\{n,l\}}\sum_{k=1}^{M}(-1)^{k+1}\rho(m,k)\int_0^\infty y\exp(-y)\\ &\left[\begin{array}{c}\sum_{v=1}^{n^{(Le)}}w_v^{(Le)}\exp\left(-\frac{k\Upsilon_m T\left[\sqrt{\frac{y}{\pi\lambda}}\sqrt{\frac{1}{2}\zeta_v^{(Le)}+\frac{1}{2}}\right]^\alpha}{SNR^{(br)}\omega_u^{\beta\sqrt{\frac{1}{2}\zeta_v^{(Le)}+\frac{1}{2}}\sqrt{\frac{y}{\pi\lambda}}}}\right)\\ \mathcal{L}\left(\frac{k\Upsilon_m T\left[\sqrt{\frac{y}{\pi\lambda}}\sqrt{\frac{1}{2}\zeta_v^{(Le)}+\frac{1}{2}}\right]^\alpha}{P^{(b)}\omega_u^{\beta\sqrt{\frac{1}{2}\zeta_v^{(Le)}+\frac{1}{2}}\sqrt{\frac{y}{\pi\lambda}}}}, \sqrt{\frac{y}{\pi\lambda}}\right)p_u\left(\sqrt{\frac{y}{\pi\lambda}}\sqrt{\frac{1}{2}\zeta_v^{(Le)}+\frac{1}{2}}\right)\end{array}\right]dy\end{aligned}$$

Utilizing the inner integral has a form of Gauss–Laguerre quadrature, $\mathcal{P}_{wo}$ is approximated as in Equation 24. Theorem 2 is proved.

H. Appendix

Since the typical user can receive the signal from the serving BS and relay via LoS and nLoS links with a probability of $p_l\left(r^{(bu)}\right)$ and $p_r\left(r^{(bu)}\right)$, $p_l\left(r^{(ru)}\right)$ and $p_r\left(r^{(ru)}\right)$ respectively. Thus, the coverage probability $\mathcal{P}_w$ is expanded as follows

$$\mathcal{P}_w = \sum_{u=\{n,l\}} \sum_{v=\{n,l\}} \mathbb{P}\left(\frac{S_u^{(bu)} + S_v^{(ru)}}{I+\sigma^2} > T\right) p_u\left(r^{(bu)}\right)) p_v\left(r^{(ru)}\right) \tag{H.14}$$

where $S_u^{(bu)} = P^{(b)} g_u^{(bu)} \omega_u^{\beta r^{(bu)}} \left[r^{(bu)}\right]^{-\alpha}$ and $S_u^{(ru)} = P^{(r)} g_v^{(ru)} \omega_v^{\beta r^{(bu)}} \left[r^{(ru)}\right]^{-\alpha}$.

Since $g^{(bu)}$ and $g^{(ru)}$ are normalized Gamma random variable with shape m and scale $1/m$ which is denoted by $\Gamma\left(m, \frac{1}{m}\right)$, $S_{uv} = S_u^{(bu)} + S_v^{(ru)}$ is the sum of two Gamma random variables which are denoted by $\Gamma\left(m, \frac{P^{(b)} L\left(r^{(bu)}\right)}{m}\right)$ and $\Gamma\left(m, \frac{P^{(r)} L\left(r^{(ru)}\right)}{m}\right)$. By utilizing Welch-Satterthwaite approximation, the S is approximated by a single Gamma random variable with a shape of p, a scale of y and a CDF of

$$F_S(x) = \int_0^x \frac{u^{p-1}}{y^p \Gamma(p)} \exp\left(-\frac{u}{y}\right) du \tag{H.15}$$

where

$$p_S = \frac{m\left[P^{(b)} L_u\left(r^{(bu)}\right) + P^{(r)} L_v\left(r^{(ru)}\right)\right]^2}{\left[P^{(b)} L_u\left(r^{(bu)}\right)\right]^2 + \left[P^{(r)} L_v\left(r^{(ru)}\right)\right]^2}; \tag{H.16}$$

$$y_S = \frac{\left[P^{(b)} L_u\left(r^{(bu)}\right)\right]^2 + \left[P^{(r)} L_v\left(r^{(ru)}\right)\right]^2}{P^{(b)} L_u\left(r^{(bu)}\right) + P^{(r)} L_v\left(r^{(ru)}\right)} \tag{H.17}$$

Thus, S can be represented as the function of the normalized Gamma random variable X. Particularly,

$$S = yX \tag{H.18}$$

where $y = m\left[P^{(b)} L_u\left(r^{(bu)}\right) + P^{(r)} L_v\left(r^{(ru)}\right)\right]$, the shape of X is $p = p_S$. As proved in the literature, the tightly upper bound of $F_S(x)$ is

$$F_S(x) = \sum_{k=0}^{M} \rho(p,k)(-1)^k e^{-k\Upsilon_p x} \tag{H.19}$$

where $\Upsilon_p = p\left[\Gamma(1+p)\right]^{-1/p}$.

Thus, the coverage probability $\mathcal{P}_w$ in Equation H.14 is re-written as follows $\mathcal{P}_w =$

$$\sum_{u=\{n,l\}} \sum_{v=\{n,l\}} \mathbb{P}\left(S > T\left(I+\sigma^2\right)\right) p_u\left(r^{(bu)}\right)) p_v\left(r^{(ru)}\right)$$

$$= \sum_{u=\{n,l\}} \sum_{v=\{n,l\}} \mathbb{P}\left(X > T\frac{\left(I+\sigma^2\right)}{y}\right) p_u\left(r^{(bu)}\right)) p_v\left(r^{(ru)}\right)$$

$$= \sum_{u=\{n,l\}} \sum_{v=\{n,l\}} \sum_{k=1}^{M} \rho(p,k)(-1)^{k+1} \mathbb{E}\left[\exp\left(-\frac{k\Upsilon_p}{y} T\left(I+\sigma^2\right)\right)\right] p_u\left(r^{(bu)}\right)) p_v\left(r^{(ru)}\right)$$

$$= \sum_{u=\{n,l\}} \sum_{v=\{n,l\}} \sum_{k=1}^{M} \rho(p,k)(-1)^{k+1} \mathbb{E}\left[\exp\left(-\frac{k\Upsilon_p}{y} T\sigma^2\right) \exp\left(-\frac{k\Upsilon_p}{y} TI\right)\right] p_u\left(r^{(bu)}\right)) p_v\left(r^{(ru)}\right)$$

$$= \sum_{u=\{n,l\}} \sum_{v=\{n,l\}} \sum_{k=1}^{M} \rho(p,k)(-1)^{k+1} \mathbb{E}\left[\exp\left(-\frac{k\Upsilon_p}{y} T\sigma^2\right) \mathcal{L}\left(-\frac{k\Upsilon_p}{y} T, r^{(ru)}\right)\right] p_u\left(r^{(bu)}\right)) p_v\left(r^{(ru)}\right)$$

The above expectation is the function of the distance from the typical user to the nearest BS and relay with the joint PDF as in Equation 1. Hence, the coverage probability is finally obtained as follows

$$\mathcal{P}_w = \sum_{u=\{n,l\}} \sum_{v=\{n,l\}} \sum_{k=1}^{M} \rho(m,k)(-1)^{k+1} \int_0^{\infty} \int_0^{r^{(ru)}} \left[\exp\left(-\frac{k\Upsilon_p}{y} T\sigma^2\right) \mathcal{L}\left(-\frac{k\Upsilon_p}{y} T, r^{(ru)}\right) p_u\left(r^{(bu)}\right) p_v\left(r^{(ru)}\right) f_{12}\left(r^{(bu)}, r^{(ru)}\right)\right] dr^{(bu)} dr^{(ru)}$$

Similarity to Theorem 2, by employing a change of variable $r^{(bu)} = r^{(ru)}\sqrt{t}$ which is followed by $y = \pi\lambda\left[r^{(ru)}\right]^2$, we obtain

$$\mathcal{P}_w = \sum_{u=\{n,l\}} \sum_{v=\{n,l\}} \sum_{k=0}^{M} \rho(p,k)(-1)^k \int_0^{\infty} \int_0^{1} \left[\exp\left(-\frac{k\Upsilon_p}{y} T\sigma^2\right) \mathcal{L}\left(-\frac{k\Upsilon_p}{y} T, \sqrt{\frac{y}{\pi\lambda}}\right) p_u\left(r^{(bu)}\right) p_v\left(r^{(ru)}\right) f_{12}\left(r^{(bu)}, r^{(ru)}\right)\right] y \exp(-y)\, dt dy$$

where

$$p = \frac{m\left[P^{(b)} \omega_u^{\beta r^{(ru)}\sqrt{t}} t^{-\alpha/2} + P^{(r)} \omega_v^{\beta r^{(ru)}}\right]^2}{\left[P^{(b)} \omega_u^{\beta r^{(ru)}\sqrt{t}} t^{-\alpha/2}\right]^2 + \left[P^{(r)} \omega_v^{\beta r^{(ru)}}\right]^2} \tag{H.20}$$

$$; y = m\left[P^{(b)} L_u\left(r^{(bu)}\right) + P^{(r)} L_v\left(r^{(ru)}\right)\right] \tag{H.21}$$

Employing Gauss–Legendre and Gauss–Laguerre quadratures for the inner and outer integrals, Theorem 3 is proved.

References

[1] 3GPP TR 38.901 version 15.0.0 Release 15, "5G; Study on channel model for frequencies from 0.5 to 100 GHz," 07 2018.

[2] S. Mukherjee and R. Chopra, "Performance Analysis of Cell-Free Massive MIMO Systems in LoS/ NLoS Channels," *IEEE Transactions on Vehicular Technology*, vol. 71, no. 6, pp. 6410–6423, 2022.

[3] Y. Lu and L. Dai, "Near-Field Channel Estimation in Mixed LoS/NLoS Environments for Extremely Large-Scale MIMO Systems," *IEEE Transactions on Communications*, vol. 71, no. 6, pp. 3694–3707, 2023.

[4] I. Atzeni, J. Arnau, and M. Kountouris, "Downlink Cellular Network Analysis With LOS/NLOS Propagation and Elevated Base Stations," *IEEE Transactions on Wireless Communications*, vol. 17, no. 1, pp. 142–156, 2018.

[5] M. Banar, A. Mohammadi, and M. Kazemi, "Characterization of mmWave X-duplex multi-relay system in 5G mobile network," *International Journal of Communication Systems*, vol. 35, no. 8, p. e5117, 2022. [Online]. Available: https://onlinelibrary.wiley.com/doi/abs/10.1002/dac.5117

[6] Y. Wang, C. Chen, H. Zheng, and X. Chu, "Performance of Indoor Small-Cell Networks Under Interior Wall Penetration Losses," *IEEE Internet of Things Journal*, vol. 10, no. 12, pp. 10 907–10 915, 2023.

[7] C.-X. Wang, X. You, X. Gao, X. Zhu, Z. Li, C. Zhang, H. Wang, Y. Huang, Y. Chen, H. Haas, J. S. Thompson, E. G. Larsson, M. D. Renzo, W. Tong, P. Zhu, X. Shen, H. V. Poor, and L. Hanzo, "On the Road to 6G: Visions, Requirements, Key Technologies, and Testbeds," *IEEE Communications Surveys & Tutorials*, vol. 25, no. 2, pp. 905–974, 2023.

[8] 3GPP TS 36.300 version 15.10.0 Release 15, "LTE; Evolved Universal Terrestrial Radio Access (E-UTRA) and Evolved Universal Terrestrial Radio Access Network (E-UTRAN); Overall description; ," 12 2019.

[9] M. Wang, W. Duan, G. Zhang, M. Wen, J. Choi, and P.-H. Ho, "On the Achievable Capacity of Cooperative NOMA Networks: RIS or Relay?" *IEEE Wireless Communications Letters*, vol. 11, no. 8, pp. 1624–1628, 2022.

[10] B. Li, D. Xu, B. Chen, and I. Ahmad, "Outage performance of CoMP-CNOMA networks with duplex mode selection," *Physical Communication*, vol. 52, p. 101701, 2022. [Online]. Available: https://www.sciencedirect.com/science/article/pii/S187449072200057X

[11] Y. Kim, J. Jeong, S. Ahn, J. Kwak, and S. Chong, "Energy and Delay Guaranteed Joint Beam and User Scheduling Policy in 5G CoMP Networks," *IEEE Transactions on Wireless Communications*, vol. 21, no. 4, pp. 2742–2756, 2022.

[12] B. Li, Y. Dai, Z. Dong, E. Panayirci, H. Jiang, and H. Jiang, "Energy-Efficient Resources Allocation With Millimeter-Wave Massive MIMO in Ultra Dense HetNets by SWIPT and CoMP," *IEEE Transactions on Wireless Communications*, vol. 20, no. 7, pp. 4435–4451, 2021.

[13] M. Elhattab, M. A. Arfaoui, and C. Assi, "Joint Clustering and Power Allocation in Coordinated Multipoint Assisted C-NOMA Cellular Networks," *IEEE Transactions on Communications*, vol. 70, no. 5, pp. 3483–3498, 2022.

[14] S. Mirbolouk, M. Valizadeh, M. C. Amirani, and S. Ali, "Relay Selection and Power Allocation for Energy Efficiency Maximization in Hybrid Satellite-UAV Networks With CoMP-NOMA Transmission," *IEEE Transactions on Vehicular Technology*, vol. 71, no. 5, pp. 5087–5100, 2022.

[15] M. Di Renzo, F. H. Danufane, and S. Tretyakov, "Communication Models for Reconfigurable Intelligent Surfaces: From Surface Electromagnetics to Wireless Networks Optimization," *Proceedings of the IEEE*, vol. 110, no. 9, pp. 1164–1209, 2022.

[16] T. V. Nguyen, D. N. Nguyen, M. D. Renzo, and R. Zhang, "Leveraging Secondary Reflections and Mitigating Interference in Multi-IRS/RIS Aided Wireless Networks," *IEEE Transactions on Wireless Communications*, vol. 22, no. 1, pp. 502–517, 2023.

[17] X. Zhang and H. Zhang, "Hybrid Reconfigurable Intelligent Surfaces-Assisted Near-Field Localization," *IEEE Communications Letters*, vol. 27, no. 1, pp. 135–139, 2023.

[18] R. Zhang, Q. Zhang, and H. Zhu, "RIS-assisted cell-free massive MIMO systems with reflection area: AP number reduction," *Physical Communication*, vol. 55, p. 101857, 2022. [Online]. Available: https://www.sciencedirect.com/science/article/pii/S1874490722001422

[19] B. Al-Nahhas, M. Obeed, A. Chaaban, and M. J. Hossain, "RIS-Aided Cell-Free Massive MIMO: Performance Analysis and Competitiveness," in *2021 IEEE International Conference on Communications Workshops (ICC Workshops)*, 2021, pp. 1–6.

[20] S. Arzykulov, G. Nauryzbayev, A. Celik, and A. M. Eltawil, "RIS-Assisted Full-Duplex Relay Systems," *IEEE Systems Journal*, vol. 16, no. 4, pp. 5729–5740, 2022.

[21] Q. Cheng, L. Zhang, J. Y. Dai, W. Tang, J. C. Ke, S. Liu, J. C. Liang, S. Jin, and T. J. Cui, "Reconfigurable Intelligent Surfaces: Simplified-Architecture Transmitters—From Theory to Implementations," *Proceedings of the IEEE*, vol. 110, no. 9, pp. 1266–1289, 2022.

[22] J. Rains, J. ur Rehman Kazim, A. Tukmanov, L. Zhang, Q. H. Abbasi, and M. A. Imran, *Practical Design Considerations for Reconfigurable Intelligent Surfaces*, 2023, pp. 99–122.

[23] P. Donegan, "New Bachhaul Requirement for LTE, LTE-Advanced & Beyond," *Heavy Reading - Juniper Networks*, 2015.

[24] S. Bassoy, H. Farooq, M. A. Imran, and A. Imran, "Coordinated Multi-Point Clustering Schemes: A Survey," *IEEE Communications Surveys & Tutorials*, vol. 19, no. 2, pp. 743–764, 2017.

[25] M. Feng and S. Mao, "Dealing with Limited Backhaul Capacity in Millimeter-Wave Systems: A Deep Reinforcement Learning Approach," *IEEE Communications Magazine*, vol. 57, no. 3, pp. 50–55, 2019.

[26] S. C. Lam and X. N. Tran, "Improving user performance in cooperative NOMA millimeter wave networks under two-phase operation protocol," *AEU - International Journal of Electronics and Communications*, vol. 170, p. 154857, 2023. [Online]. Available: https://www.sciencedirect.com/science/article/pii/S143484112300331X

[27] Z. Chen, J. Yuan, and B. Vucetic, "Analysis of transmit antenna selection/maximal-ratio combining in Rayleigh fading channels," *IEEE Transactions on Vehicular Technology*, vol. 54, no. 4, pp. 1312–1321, 2005.

[28] M. Haenggi, *Stochastic Geometry for Wireless Networks* . Cambridge Univ. Press, November 2012.

[29] H. Alzer, "On some inequalities for the incomplete gamma function," *Mathematics of Computation*, vol. 66, no. 218, p. 771–778, 1997.

[30] T. Bai, R. Vaze, and R. W. Heath, "Analysis of blockage effects on urban cellular networks," *IEEE Transactions on Wireless Communications*, vol. 13, no. 9, pp. 5070–5083, 2014.

[31] W. Jiang, B. Han, M. A. Habibi, and H. D. Schotten, "The Road Towards 6G: A Comprehensive Survey," *IEEE Open Journal of the Communications Society*, vol. 2, pp. 334–366, 2021.

[32] A. Jeffrey, D. Zwillinger, I. Gradshteyn, and I. Ryzhik, *Table of Integrals, Series, and Products (Seventh Edition)*. Academic Press, 2007.